JOURNAL OF PROPULSION AND POWER
Vol. 10, No. 6, Nov.–Dec. 1994

Multifunction Droplet Imaging and Velocimetry System for Spray Jets

Tzong H. Chen,* Larry A. Roe,† and Abdollah S. Nejad‡
Wright Laboratory, Wright-Patterson Air Force Base, Ohio 45433

The development of a multifunction instrumentation system capable of scalar imaging and velocity-vector mapping of a dense liquid jet in crossflow is described. This system requires only one laser that is double-pulsed to produce droplet-displacement images. Direct image digitization and processing using a combination of a charge-coupled device camera, controller, microcomputer, and custom software has shortened the image-processing time from days to minutes. Important features of this effective image-analysis process include 1) a high-speed, general-purpose scheme capable of analyzing image size and shape factor, therefore determining droplet location; 2) a rapid method of computing two-dimensional spatial correlation; 3) a compact data structure for merging image-intensity and geometry information to reduce data storage and improve tracking accuracy; and 4) a newly developed three-point interpolation scheme that preserves the two-dimensional vector field for postprocessing. Application of this imaging system to the study of liquid jets transversely injected into a crossflow has yielded a much improved formulation that takes into account multizone jet behavior in describing jet penetration into the crossflow. The measurement of droplet and spray fragment velocities throughout the spray field indicated substantial droplet-freestream velocity slip even at far-downstream locations.

Introduction

MOST laser-based diagnostic instruments are severely limited when applied to the dense regions of fuel spray. The flowfield is turbulent and two-phase in nature. The liquid phase could also be in the form of spray fragments rather than spherical droplets. In addition, the liquid phase can be associated with complicated transition phenomena. This problem becomes even more complicated when combustion is involved. The majority of earlier investigations were directed at giving global and qualitative information about the spray. For example, flow visualization, pattern characterization, and integrated line-of-sight droplet-size-distribution measurements were performed by using high-speed photography, mechanical probes, and laser light diffraction techniques. In the meantime, the development and validation of numerical codes that can correctly account for droplet-turbulence interaction and species transport call for detailed flow statistics such as gas-phase velocity and droplet size/velocity distribution. There are commercial instruments available such as laser Doppler anemometry (LDA) and the phase Doppler particle analyzer (PDPA) that can be utilized. However, in the dense spray regions, both LDA and PDPA encounter signal saturation, deterioration, and discrimination problems that result from irregular droplet shape, dense droplet population, and a wide range of droplet size distribution. Skillful experimentalists may be able to perform some velocity/size measurements in the dense flow region. The measured results will, however, depend upon the instrumentation parameters[1–3] and lead to difficulty in interpreting the data. A typical example is improper PMT voltage settings that can bias the results toward a particular size group of the seeding material or the droplets.

Presented as Paper 93-0415 at the AIAA 31st Aerospace Sciences Meeting and Exhibit, Reno, NV, Jan. 11–14, 1993; received Jan. 30, 1993; revision received Feb. 28, 1994; accepted for publication March 7, 1994.

*Taitech Group, Advanced Propulsion Division, Aero Propulsion and Power Directorate WL/POPT.

†Department of Mechanical Engineering; currently University of Arkansas, Fayetteville, AR 72701.

‡Aerospace Engineer, Advanced Propulsion Division, Aero Propulsion and Power Directorate, WL/POPT.

While the joint effort between spray measurement and modeling is in its early stage of development, the role played by flow visualization in helping the engine design processes is still invaluable. Among various flow measurement techniques, particle image velocimetry (PIV)[3–6] has several advantages. PIV is a combination flow visualization and velocity mapping tool that uses a laser as the versatile light source. It involves taking double-pulsed images of particles traveling in the flowfield to determine the particle displacement, and therefore, the velocity. The temporal resolution is determined by the laser pulse separation that can be precisely adjusted to accommodate the velocity range of interest. The individual laser pulse, e.g., from an Nd:YAG laser, is typically 8 ns wide, which is sufficiently short for instantaneous flowfield mapping. Traditionally, PIV techniques use film for recording the images that then require digitization or other postoptical processing to obtain the particle displacement information. Recent advances in charge-coupled device (CCD) technology enable direct digitization and downloading of a large number of pixel images into the computer memory. The memory capacity and speed of current technology are capable of accommodating the throughput and storage of the imaged field. For image analysis and display, the CPU power of modern microcomputers and workstations is well-suited for practical application.

In this study, several techniques were adapted to make PIV more efficient, affordable, and easy to implement. The velocity determination with PIV is predominantly controlled by pixel resolution and the separation time between laser pulses. Therefore, no system calibration and recalibration are needed, provided that the above two quantities are properly set and monitored. Therefore, to test the software and hardware, the system was directly applied to the spray environment. In order to explore the significance of the measured data, comparisons were made with a computational study as well as data obtained using a PDPA system. Results of the comparison are reported.

System Development Strategies and Procedures

A schematic of the PIV system and the fuel injection tunnel is depicted in Fig. 1. The multifunction imaging and droplet velocimetry system described here includes a Nd:YAG laser, CCD camera, controller, and a microcomputer. The 532-nm line of a double-pulsed Quanta-Ray DCR-3 Nd:YAG laser

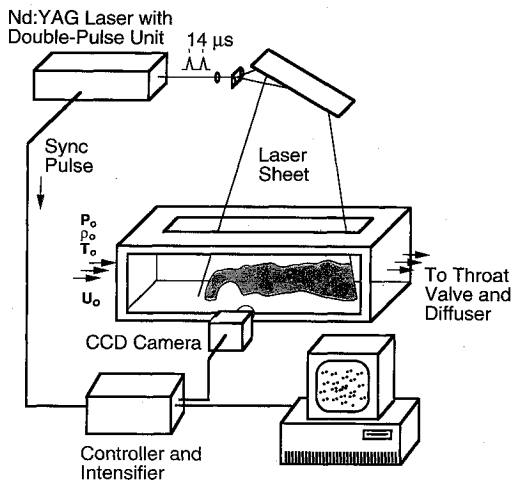

Fig. 1 Experimental setup of PIV system around fuel injection tunnel.

is used as the light source. A thin (1-mm-thick) laser light sheet was formed by a combination conventional/cylindrical lens system. The light sheet was longitudinally oriented and passed through the window on the top wall of the test section to illuminate the spray at the plane of symmetry. The scattered light (Mie scattering from the droplets and spray fragments) was collected at 90 deg off axis by an intensified two-dimensional CCD camera (Princeton Instruments Model 576S/B). The 384 × 576 pixel density of the CCD camera combined with the optical arrangement resulted in a 200-μm/pixel spatial resolution (coarse resolution), which allowed the observation of a 76.8 × 115.6 mm area of interest. For the velocity mapping, the camera was zoomed to yield a 32-μm/pixel spatial resolution (fine resolution), which allowed observation of a 12.4 × 18.6 mm area. The duration of each pulse was 8 ns, which was sufficiently short to freeze the flow and act as an optical shutter. The optimal time separation for the double Q-switching is ~100 μs. However, with moderate care and adjustment of the Q-switch delay, it was possible to obtain 14-μs pulse separation. Thus, the velocity resolution of this double-pulsed, single-laser velocimetry system is roughly 2.3 m/s per pixel. To capture light scattering from both laser pulses, the gate width of the intensifier was set at ~15 μs.

Each image acquired by the CCD camera was sent to a 486-PC through a controller unit for preliminary analysis and display. For each pixel, the light intensity resolution was 14 bits. For storage, the image data were rescaled to 12 bits, i.e., maximum value of 4095. The remaining four bits could then be used for storing droplet-size information for droplet image velocimetry. This confines the information associated with each pixel to a 16-bit (two-byte word) limit that is the binary data format adopted by Princeton Instruments. Thus, each raw-image data set contains 440 KBytes of information.

In a separate effort for determining the jet trajectory, a set consisting of 10 individual images was acquired for each flow condition. These images were sent to a Macintosh IIfx computer for analysis through data conversion by custom software developed in this study. These images were averaged and used to determine the jet penetration by outlining the spray-plume boundary and to obtain the time-averaged behavior of the jet. A computer program was written to identify the trajectory of the spray plume based upon the assumption that the jet boundary has a 10% maximum field intensity, similar to the convention used for defining boundary-layer height. The upper part of this contour line is considered to be the penetration height. Approximately 400 data points were obtained to describe the upper jet contour, which typically extended to 70 jet diameters downstream of the injector orifice. The present sheet-lighting technique together with the ability to digitize the images has markedly improved the accuracy of measurements for determining the jet trajectory. The result is a much improved formulation[7] which takes into account the multizone jet behavior in describing jet penetration in crossflow. A precise description of the jet trajectory is especially important for future modeling efforts.

For velocity mapping, several innovative steps have been taken to shorten the data processing time from days to minutes. The images were directly digitized and stored in the computer using the binary format described above. This allows further manipulation of data using custom software. Under some circumstances, high-pass filtering of the acquired data may be required to enhance the droplet images. For the convolution calculation using a 3 × 3 high-pass filter mask, approximately 1 min is required on a Macintosh IIfx computer (without array processor); this is the most time-consuming step. A level-searching routine was developed for tracking the droplet image to yield geometric information such as image area (can be related to droplet size), circumference, and mass center.[8] This additional information greatly enhanced the pairing process of the displaced droplets. Typically, about 13 s are required for the determination of the droplet locations in an image composed of roughly 6000 droplets.

Before initiating the pairing process, a two-dimensional, spatial-correlation calculation was performed to determine

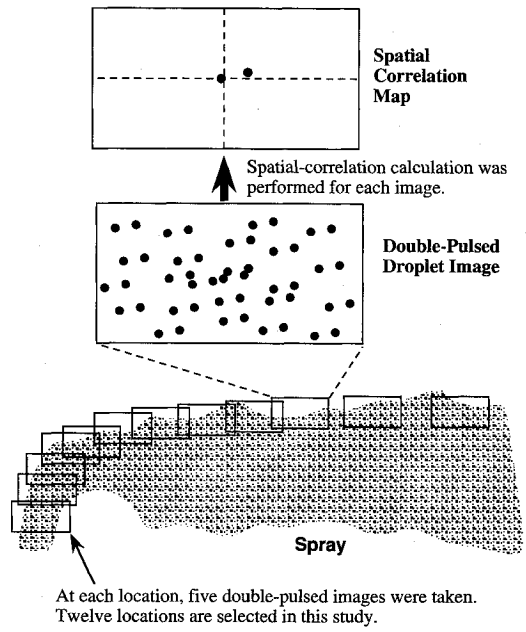

Fig. 2 Diagram of PIV data acquisition and analysis processes.

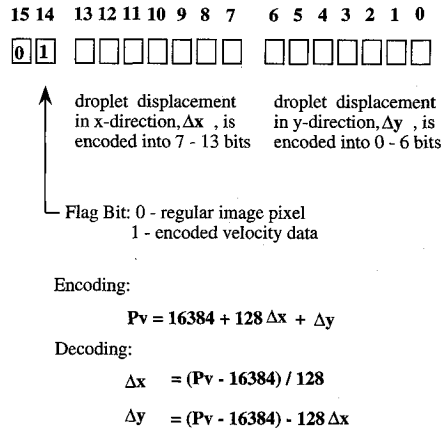

Fig. 3 Encoding and decoding scheme enables packing of two-component velocity into 16-bit data structure.

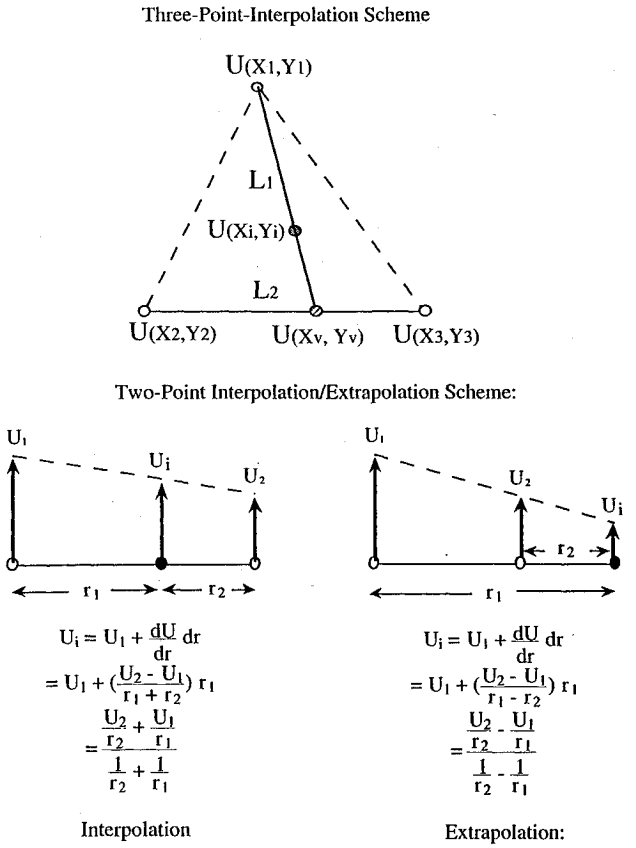

Fig. 4 Three-point interpolation scheme.

the most probable droplet displacement as shown in Fig. 2. This most probable displacement indicates the mean global droplet velocity. To reduce the time required for correlation calculations, a forward-looking scheme was used due to the fact that the correlation is symmetrical with respect to the reference zero. In addition, only the pixel depicting the mass center of the droplet was used for correlation computation. This calculation requires around 10 s CPU time on the Macintosh IIfx computer. After the most probable droplet displacement was determined, the information was then used to perform the pairing process on the droplet image map. In this pairing process, the droplet size (from the level searching routine) and the pixel intensity (from the image itself) were also used to reduce the pairing ambiguity. This pairing process requires about 2 s of CPU time. Once the displacement vector was found, the displacement information was encoded into the lower 14 bits of the two-byte data structure configuration that originally contained the intensity associated with the mass center of the droplet. The decoding and encoding of the displacement is illustrated in Fig. 3. When the image display routine sees the data, it displays the original droplet image with saturated intensity at the droplet mass center. On the other hand, the velocity processing routine can read the same data file and can determine if a velocity pair has been found in each pixel space by examining the 14th bit (the 15th bit is always set at 0). This procedure allows the usage of a unified file structure, reduces storage space and avoids the multiple-file access requirement that is one of the major burdens of image processing. This unique step is also responsible for dramatically reducing the development time of the image processing software.

Under very dense spray conditions such as in the near-field region, locating the droplet becomes more difficult, even with the aid of high-pass filtering. In addition, measurable droplets may not be available in large numbers. Inevitably, sparse pairing of the velocity vector will result. Velocity interpolation then becomes a necessity. One of the most popular forms of interpolation was described[9,10] as follows. The velocity component $U(x)$ on the grid point are calculated by Eq. (1)

$$U(x) = \sum \alpha_i U_i \Big/ \sum \alpha_i$$
$$\alpha_i = \exp(-|x - x_i|^2/H^2) \tag{1}$$

where H is the window width chosen for effective interpolation. The value of H may be the radius of the physical length scale such as the width of the recirculation zone or the characteristic size of the eddy. Another technique was reported[11] as follows. The relation between the velocity component U at a mesh point (x, y) and the velocity component U_i at a measured point (x_i, y_i) near the mesh point is expressed in Eq. (2)

$$U_i = U + \frac{\partial U}{\partial x}(x_i - x) + \frac{\partial U}{\partial y}(y_i - y) \tag{2}$$

Normally, three measured points near the mesh point were used to establish three equations in order to yield the velocity U at the mesh point. This second method preserves the two-dimensional information because it uses the velocity gradient in both directions. Since the scheme is only first-order accurate, large errors may result when measured velocity points close to the mesh point are not available. In addition, when more than three particles are available, implementation of this scheme becomes tedious. For the first method, the availability of more particles would not cause additional programming difficulties. Instead, it will smooth out the spatial fluctuations. However, the first method does not preserve two dimensionality.

In this study, a three-point interpolation scheme was explored. This scheme is capable of preserving the two dimensionality as illustrated in Fig. 4. The purpose of this scheme is to find the value at point (X_i, Y_i) based on the known values at three nearby points: (X_1, Y_1), (X_2, Y_2), and (X_3, Y_3). The procedure steps involved are as follows: 1) pair (X_i, Y_i) with a known point, e.g., (X_1, Y_1), to form a line, L_1; 2) pair the other two known points, i.e., (X_2, Y_2) and (X_3, Y_3), to form a line, L_2; 3) find the intersection of L_1 and L_1: (X_v, Y_v); 4) use a two-point interpolation/extrapolation scheme to find value $U(X_v, Y_v)$, based on values of $U(X_2, Y_2)$ and $U(X_3, Y_3)$; and 5) use a two-point scheme to find the value $U(X_i, Y_i)$ based on values of $U(X_1, Y_1)$ and $U(X_v, Y_v)$.

The result of this three-point interpolation scheme has characteristics of the method adapted by Tsurusaki and Urata[11] with the added advantage of simple programming requirements. However, a sorting routine using the information of particle locations to select the three nearest measured points is required and was implemented. The first method of Agui and Jimenez[9] can be used to cross-check the interpolated results. If the difference between these two schemes is greater than a set deviation, then the sorting routine will be used again for selecting a different three-point set. The test results indicated that under the sparse data environment, data interpolation is sensitive to the measurement uncertainty. It seems that using both methods for cross-checking may be the best way to perform data interpolation.

System Validation

Numerical Simulation

To better understand the performance characteristics of the PIV system developed in this study, a simple numerical simulation was performed to yield droplet trajectory for comparison. The fourth-order Runge-Kutta method was applied

to solve the equations governing droplet motion through air as follows[12]:

$$\frac{d^2x}{dt^2} = \frac{3\bar{\rho}}{4d} C_d(u_f - u)w_r \Big/ \left(1 + \frac{1}{2}\bar{\rho}\right)$$

$$\frac{d^2y}{dt^2} = \left[-(1 - \bar{\rho})g + \frac{3\bar{\rho}}{4d} C_d(v_f - v)w_r\right] \Big/ \left(1 + \frac{1}{2}\bar{\rho}\right) \quad (3)$$

$$w_r = \sqrt{(u_f - u)^2 + (v_f - v)^2}$$

$$\bar{\rho} = \frac{\rho_f}{\rho}$$

where d is droplet diameter, C_d the drag coefficient, u_f streamwise gas velocity, v_f vertical gas velocity, u streamwise droplet velocity, and v vertical droplet velocity. The droplet velocity variation as a function of time and x-y space, i.e., trajectory, was obtained from this computation. The trajectories for droplets with sizes ranging from 1 to 300 μm were computed. The drag coefficient is set as a function of Reynolds number. For the present computation, vaporization is not considered so that d is constant during each calculation.

Velocity/Size Measurements

The PDPA system, developed by Aerometrics Inc., was used for in situ size and velocity measurements. The detailed theory of PDPA is described.[13] Briefly, it is a single-component laser Doppler anemometer (LDA) with multiple photodetectors and additional signal processing capability. As an LDA system, it is of the standard dual-beam type. Two laser beams intersect at a small angle in the region where measurements are to be obtained. The crossing of these two beams forms a probe volume. The frequency modulation of the scattered light from particles passing through the probe volume is a function of the transmitting optics and the droplet velocity. The scattered light is detected by a PMT and then processed to obtain the velocity information. For the droplet sizing, additional information from two other PMTs is required. The PMTs all observe the same temporal frequency (the Doppler frequency related to velocity) but will observe phase differences that can be related to the droplet diameter.

Determination of the operational characteristics of the PDPA was performed.[14] The overall system accuracy was estimated to be approximately 7% for mean velocity and 5% on diameter for droplets larger than 2 μ. In addition, the effects of the primary instrument operating parameters upon the measurements were examined. The most consistent source of error was found to be the PMT supply voltage setting, which if improperly set can bias the measured velocity and size. This has been reported by other researchers.[1] It was found that a PMT voltage setting below 320 V gave very truncated size distributions, with essentially no sensitivity to droplets smaller than about 15 μ. A supply voltage above 380 V caused an excessive sensitivity to droplets smaller than the 2–3 μ, which is the low limit for which full measurement confidence has been established. Since a major portion of the spray mass is associated with large droplets and the breakup of these droplets is the primary concern of the injection studies, an operating PMT voltage of 350 V was established for the spray experiments. It was realized, however, that some adjustment to this may be required when probing different regions of the spray plume. This system was then used to measure the droplet velocity and size for the test condition with an air velocity of Mach 0.2 (68 m/s) and a water flow rate of 0.381 kg/min through an injector of 0.76-mm diam. Frequency shifting of 20 m/s was applied to the incident beams to expand the available range of velocities. The spray cross section was fully mapped at 2.0 and 5.0 in. downstream of the injector, and vertical centerline profiles were measured at 0.5, 1.0, 3.0, 4.0, and 6.0 in.

Results and Discussion

In this section, the test results of a liquid (water) jet injected into the crossflow airstream at Mach 0.2 are discussed. The velocities measured by PIV and by PDPA are presented here for comparison. To aid the understanding of the droplet trajectory in the crossflow, a numerical calculation was performed and the results are also presented.

Several locations (see Fig. 2) along the jet spray were selected for the PIV measurement. Figure 5 depicts a typical double-exposed image of the droplet field. Since the technique for locating the droplet image involves interrogation of

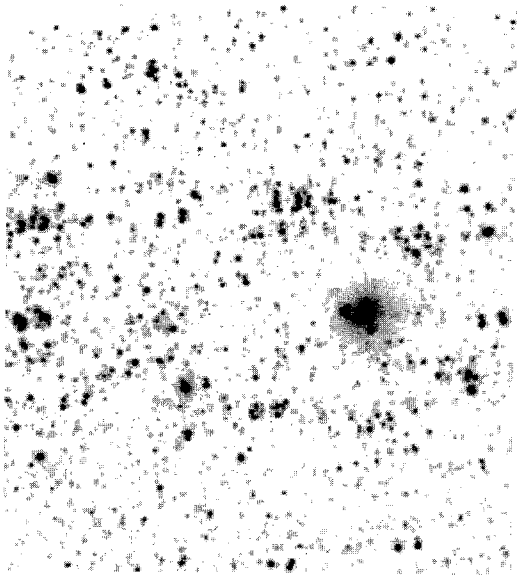

Fig. 5 Image of droplet displacement captured by double-pulsed laser light.

Fig. 6 Enhanced droplet image using high-pass filtering.

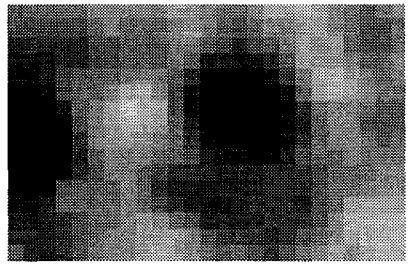

Fig. 7 Spatial correlation map to determine droplet displacement.

the intensity level, the elimination of the background signal is often needed. The image data shown on Fig. 5 were high-pass filtered to eliminate the background light as is shown in Fig. 6. Comparing Figs. 5 and 6 demonstrates that the "visibility" of the droplet image field was greatly enhanced by the high-pass filtering process.

Spatial correlation calculations can be performed on the original or the filtered image. The resulting correlation coefficient as a function of spatial displacement was converted into intensity so that the correlation map can be stored using the same file format as the original image. The resulting correlation map that represents the global droplet displacement is shown in Fig. 7 as an example. If only the global (spatial averaged) velocity measurement is required, then the original droplet image can be used for spatial correlation calculations to yield smoother correlation maps as shown in Fig. 7. The smooth map makes the task of locating the peak of the correlation (using level searching techniques) extremely easy. If velocity information is needed, then only the pixel related to the mass center of the droplet image will be involved in the correlation calculation. This will dramatically reduce the processing time for the correlation calculation. On the other hand, since the samples for the correlation calculation are only limited to the pixel associated with the droplet center, the undersampling situation results in a coarse correlation map. Under this circumstance, the intensity level searching technique may not be applicable for locating the correlation peak. However, the correlation intensity around the peak can be directly related to the two-dimensional joint velocity probability density function (PDF).

The displacement of the peak with respect to the origin of the correlation map is usually referred to as the mean global droplet displacement and can be related to the mean global velocity. This quantity is then used in the search for droplet-image pairs. The paired droplets were linked by a straight line as is shown in Fig. 8. As was pointed out in the previous section, the entire image represents an area of 12.4 × 18.6 mm. If a large velocity variation exists over the image area, then the image can be divided into subdivisions for correlation calculation and velocity pairing. In Fig. 8, it can be found that at least four pairs of velocity vectors were identified for the irregularly shaped liquid ligaments. This indicates that the pairing process using shape factor, image area, and image intensity as the criteria is working well in the spray environment where the droplet is not always spherical, which is a severe limitation for other laser diagnostic instrumentation.

The measured mean velocity along the jet boundary is displayed in Fig. 9. The freestream velocity, 68 m/s, was measured by an LDA system using Al_2O_3 as seeding material. The velocity difference between droplets and airstream is very large initially, suggesting that the droplets are accelerating under the influence of the drag force. After the initial velocity surge, the droplet then gradually approaches the freestream velocity at a much slower rate. Since this was the first time that this developed system was applied to a fuel injection study, the following comparisons were made to explore the significance and accuracy of the PIV data.

The computational results obtained for droplet diameters of 100, 150, 180, 200, and 300 μm along with the PIV data are plotted in Fig. 10. It was found that the computed velocity for the single droplet with diameter of 180 μm compares very well with the measured PIV data of the droplets in the spray. The near perfect matching between the measured data and computational results may indicate that the droplet in the spray behaves like a single droplet. However, this interesting comparison and the associated speculation can only be used for reference purposes. Before a solid conclusion can be drawn, far more detailed studies are needed.

For the purposes of comparison, only a small portion of the measured PDPA data will be presented here. Overall, it was observed that the largest droplets were generally distributed on the outer portion of the spray jet. This observation

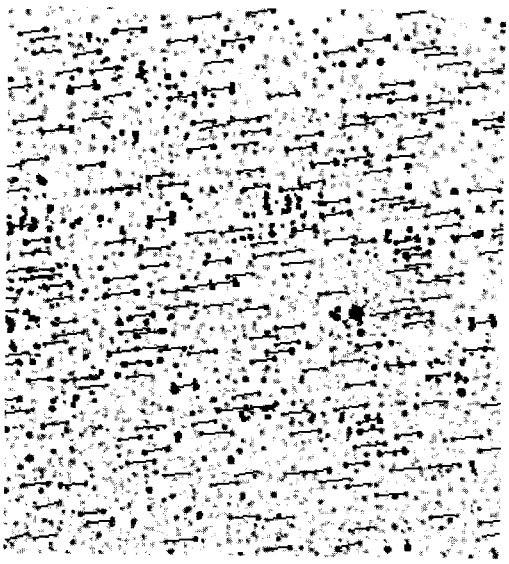

Fig. 8 Droplet-image pairing to form velocity vector using image size and intensity information.

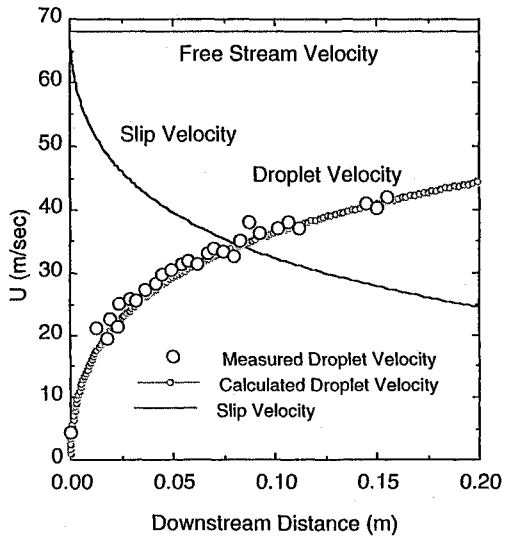

Fig. 9 Measured mean global velocity along jet boundary using PIV.

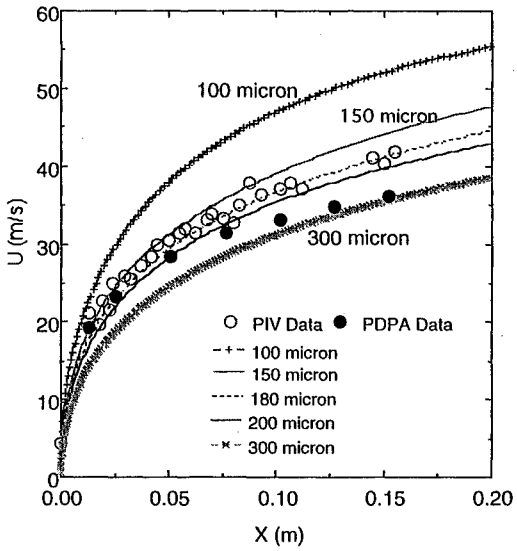

Fig. 10 Comparison of measured and computed droplet velocity.

is consistent with the earlier studies[7] using laser-sheet imaging. For velocity data comparison, the software of the Aerometrics PDPA system allows the velocity averaging to be conditioned by the droplet size. The average velocity associated with the 183-μ range is plotted in Fig. 10 along with the PIV and computed result. Good agreement among the PIV data, computed results, and PDPA data can be found in the initial jet region. However, at the downstream location, the PDPA data deviates away from both the computed and PIV data. The reason for this disagreement deserves further careful study.

Conclusions

A simple, low-cost (one laser) double-pulsed, multifunction, multipurpose PIV system capable of velocity and size determination in dense spray regions was developed and applied to study the droplet motion of a liquid jet in a high-speed crossflow environment. The robust data processing strategy developed for droplet searching, correlating, and pairing have significantly reduced the CPU processing time. The pairing process using shape factor, image area, and image intensity as the criteria also works well in the spray environment where the droplet is not always spherical. Therefore, for the first time, velocity measurements can be made in the fragment region of a spray plume. The simplified and effective process has made the PIV system more affordable for routine testing of fuel sprays. Real-time data processing is possible if an array processor is added to the Macintosh IIfx computer.

Comparison of the measured data and numerical simulation indicates that large droplets resulting from injection of liquids into a high-speed crossflow act very similar to isolated single droplets. The droplets exhibited a rather large velocity slip at far-downstream distance. The velocity data acquired with the commercially available PDPA system and the simple numerical calculation were in good agreement, except for the downstream region, with the results obtained by the PIV system.

Future work will apply and upgrade the system to study the near-field effects on breakup and atomization processes.

Acknowledgments

This work was performed at and supported by Wright Laboratory, Aero Propulsion and Power Directorate, Wright-Patterson Air Force Base, Ohio, under USAF Contracts F33615-92-C2202 and F33615-93-C-2300. The authors would like to thank L. Goss, D. Trump, D. Schommer, and C. Smith for technical assistance, and G. Switzer and M. Gruber for useful discussion.

References

[1]McDonell, V. G., and Samuelsen, G. S., "Data Quality Control Evaluation of the Aerometrics Two-Component Phase Doppler Interferometer," Univ. of California, UCI-ARTR-91-1, Irvine, Irvine, CA, July 1991.

[2]McDonell, V. G., Samuelsen, G. S., Wang, M. R., Hong, C. H., and Lai, W. H., "Interlaboratory Comparison of Phase Doppler Measurements in a Research Simplex Atomizer Spray," AIAA Paper 92-3233, 1992.

[3]Switzer, G. L., Obringer, C. A., Nejad, A. S., and Jackson, T. A., "The Influence of Particle Size on the Measurement of Turbulence Characteristics in Two Phase Flows," First Annual Conf. on Liquid Atomization and Spray Systems, International Conf. on Liquid Atomization and Spray Systems Americas 87, Madison, WI, June 1987.

[4]Adrian, R. J., "Applications of Particle Image Velocimetry," *Flow Visualization*, edited by B. Khalighi, M. J. Braun, and C. J. Freitas, American Society of Mechanical Engineers, FED-Vol. 85, New York, 1989, pp. 23–28.

[5]Goss, L., Post, M., Trump, D., Sarka, B., Dunning, G., and MacArthur, C., "A Novel Technique for Blade to Blade Velocity Measurement in a Turbine Cascade," AIAA Paper 89-2691, 1989.

[6]Molezzi, M. J., and Dutton, J. C., "Development and Application of a Particle Image Velocimeter for High-Speed Flows," AIAA Paper 92-0004, Jan. 1992.

[7]Chen, T. H., Smith, C. R., Schommer, D. G., and Nejad, A. S., "Multi-Zone Behavior of Transverse Liquid Jet in High Speed Flow," AIAA Paper 93-0453, 1993.

[8]Chen, T. H., Nejad, A. S., Carter, C. D., and Goss, L. P., "A Technique for Simultaneous Velocity Measurement of Liquid and Gas Phases," AIAA Paper 94-0494, 1994.

[9]Agui, J. C., and Jimenez, J., "On the Performance of Particle Tracking," *Journal of Fluid Mechanics*, Vol. 185, 1987, pp. 447–468.

[10]Kobayashi, T., Saga, T., and Sekimoto, K., "Velocity Measurement of Three-Dimensional Flow Around Rotating Parallel Disks by Digital Image Processing," *Flow Visualization*, edited by B. Khalighi, M. J. Braun, and C. J. Freitas, American Society of Mechanical Engineers, FED-Vol. 85, New York, 1989.

[11]Tsurusaki, H., and Urata, T., "A Measuring Method for Three-Dimensional Steady Flow by Digital Image Processing of Pathline Pictures," *Flow Visualization*, edited by B. Khalighi, M. J. Braun, and C. J. Freitas, American Society of Mechanical Engineers, FED-Vol. 85, New York, 1989.

[12]Chow, C.-Y., *An Introduction to Computational Fluid Mechanics*, Wiley, New York, 1979.

[13]Bachalo, W. D., Breña de la Rosa, A., and Sankar, S. V., "Diagnostics for Fuel Spray Characterization," *Combustion Measurements*, edited by N. Chigier, Hemisphere, Washington, DC, 1991.

[14]Roe, L. A., "Determination of the Operational Characteristics of a Phase-Doppler Droplet Analyzer and Application to a Ramjet Fuel-Injection Research Tunnel," Final Rept. for Summer Research Program, Advance Propulsion Div., Wright Labs., Wright-Patterson AFB, OH, Sept. 1992.